Journal of Materials Science & Technology 69 (2021) 42–47

Contents lists available at ScienceDirect

Journal of Materials Science & Technology

journal homepage: www.jmst.org

Research Article

Defects activation in CoFe-based metallic glasses during creep deformation

Zhuwei Lv [a], Chenchen Yuan [a,*], Haibo Ke [b], Baolong Shen [a,*]

[a] School of Materials Science and Engineering, Jiangsu Key Laboratory for Advanced Metallic Materials, Southeast University, Nanjing, 211189, China
[b] Songshan Lake Materials Laboratory, Dongguan, 523808, China

ARTICLE INFO

Article history:
Received 26 April 2020
Received in revised form 15 May 2020
Accepted 10 June 2020
Available online 7 August 2020

Keywords:
Plasticity
Creep
Disordered
Structure
Metallic glasses

ABSTRACT

Maxwell-Voigt model with two Kelvin units and one Maxwell unit was utilized to analyze the microalloying effect of Cu on the creep behavior of CoFe-based metallic glasses at different loading rates. The defect activation during creep deformation was detected by the relaxation time spectrum based on this model. The defect, with respect to a short relaxation time in relaxation spectra, intends to be activated at a quasi-static loading mode in the alloy with 0.5 at.% Cu addition. With further increasing loading rates, more defects with a large size were provoked activated at both hard and soft regions in the Cu-containing sample. A softening with the reduction of elastic modulus and hardness about 10 % and 15 %, respectively, was also observed in the Cu-doped sample. It is consistent with the pronounced viscoplastic deformation of this alloy along with the decrease of viscosity. Our work provides a microscopic insight into structural evolution during creep deformation in a Cu-doped metallic glass, which might help for understanding the plastic deformation of metallic glasses upon a minor addition.

1. Introduction

Metallic glasses (MGs), or amorphous alloys, have attracted much attention as structural or functional materials due to their outstanding mechanical properties and corrosion resistance [1,2,3]. Mechanical properties of MGs are proposed to depend on quenched-in flow defects that are frozen from their liquid structure during the rapid cooling process. It is always affected by cooling rate [4], residual stresses [5], and a minor addition [6], etc. Nanoindentation creep as time-dependent plastic deformation is frequently used to analyze the motion/diffusion of atoms involving the activation of flow defects during the plastic deformation in many MGs, for example, Al- [7], Pd- [8], Ni-[9], CuZr-[10,11], Zr-[12], TiZrHfBeCu(Ni)-[13] and Fe-based [14, 15, 16] MGs.

It has been reported that the addition of Cu element can significantly enhance the mechanical performance [6,17–19] and soft magnetic properties [20,21] of Co/Fe-based MGs. It stimulates the nucleation and refinement of α-(Co, Fe) grains [22,23], owing to the positive mixing enthalpy between Cu and Co/Fe ($\Delta H_{\text{Cu-Co}}$ = +6 kJ mol^{-1}, $\Delta H_{\text{Cu-Fe}}$ = +13 kJ mol^{-1}) [24]. Some studies point out that the atomic-scale heterogeneity existing in the glassy matrix due to the appearance of sub-nanoscale Cu rich cluster benefits the creation of a large number of flow defects, i.e. shear transformation zones [25]. It promotes the generation of plenty of excess free volumes [14] as well as the energy dissipation [26] during the plastic deformation, and leads to large compressive plasticity of MGs [23,24]. However, the convincing experimental evidence for such atomic-scale structural evolution in Cu-doped MGs during deformation is still missing.

In this work, Maxwell-Voigt model with two Kelvin units and one Maxwell unit was utilized to analyze the creep behavior of $[(Co_{0.7}Fe_{0.3})_{0.68}B_{0.219}Si_{0.051}Nb_{0.05}]_{100-x}Cu_x$ (x = 0, 0.5) MGs at ambient temperature in virtue of nanoindentation techniques. We found that adding 0.5 at.% Cu element in CoFe-based MGs can stimulate the generation of a large number of activated defects at both soft and hard regions during creep deformation, which might be the underlying reason for the improved plasticity and creep ability of Cu-doped Co/Fe-based MGs.

2. Experimental

Master alloy ingots with nominal composition $[(Co_{0.7}Fe_{0.3})_{0.68}B_{0.219}Si_{0.051}Nb_{0.05}]_{100-x}Cu_x$ (x = 0, 0.5) (denoted as Cu0 and Cu0.5) were prepared by arc-melting mixtures of pure elements (≥ 99.95 %) in a high-purity argon atmosphere. Nanoin-

* Corresponding authors.
E-mail addresses: yuanchenchenneu@hotmail.com (C. Yuan), blshen@seu.edu.cn (B. Shen).

https://doi.org/10.1016/j.jmst.2020.08.012
1005-0302/

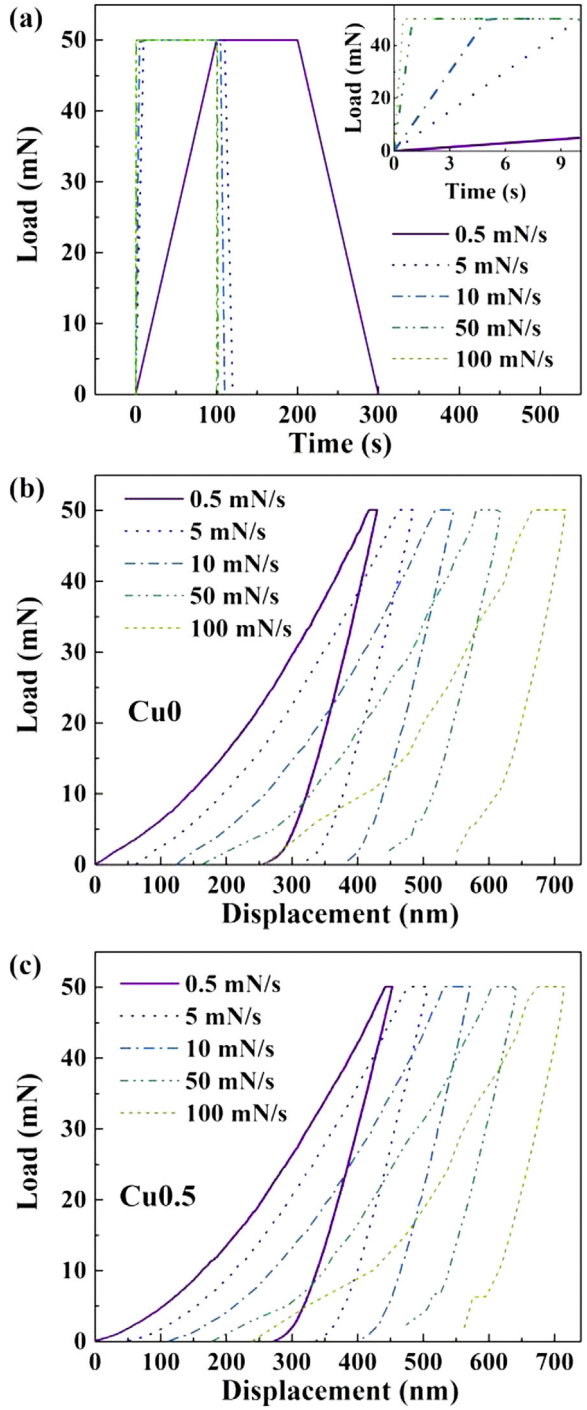

Fig. 1. (a) Load-time scheme for creep tests on CoFe-based MGs with different loading rates; the typical load-displacement (*P*-*h*) curves of Cu0 (b) and Cu0.5 (c) MGs at different loading rates under a maximum load of 50 mN.

dentation experiments were performing at room temperature by using the NanoTest Vantage (Micro Materials Ltd) with a standard Berkovich diamond indenter. Cylindrical rods with a diameter of 1 mm for indentation were fabricated by casting in a copper mold. The top surface of rod specimens was mechanically polished to a mirror-like finish. Creep measurements were conducted according to the following sequence as shown in Fig. 1(a): firstly, the sample was loaded to a limit of 50 mN with constant loading rates of 0.5, 5, 10, 50 and 100 mN/s; and then held 100 s at its load limit; finally unloaded at the same rate as loading rate.

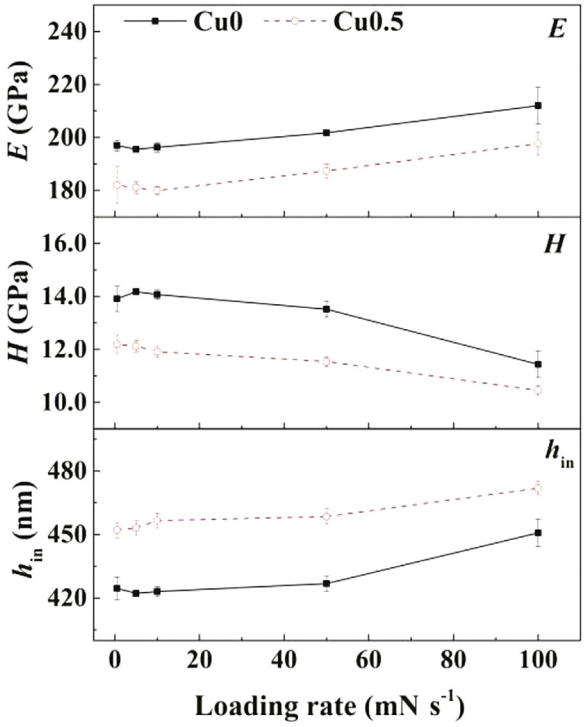

Fig. 2. Elastic modulus *E*, hardness *H*, and the maximum indentation creep h_{in} of Cu0 and Cu0.5 MGs measured at different loading rates.

3. Results and discussion

Fig. 1(b) and (c) displays the typical load-displacement (*P*-*h*) curves of Cu0 and Cu0.5 MGs at a load limit of 50 mN. No notable serration behavior is found during loading or unloading processes. Fig. 2 shows mechanical parameters derived from nanoindentation experiments of Cu0 and Cu0.5 MGs as a function of loading rates. With increasing loading rates, the elastic modulus (*E*) increases gradually from 197 to 212 and 182 to 198 GPa, while the hardness (*H*) slightly decreases from 14 to 11 and 12 to 10 GPa for Cu0 and Cu0.5 MGs, respectively. As shown in Fig. 2, the standard error of *E* is over 8% at very low or high loading rates such as 0.5 and 100 mN/s, which is much larger than that of *H* (less than 5%). The change of *E* as a function of loading rate under the studied loading condition is less than 7.5 %, thereby, *E* can be considered as a constant within the error bar. However, after adding 0.5 at.% Cu to CoFe-based MGs, the *E* and *H* are significantly reduced by about 10 % and 15 %, respectively. For instance, the *E* and *H* drop from 196 to 180 and 14 to 12 GPa, respectively, with the addition of Cu at the loading rate of 10 mN/s. It suggests that the softening of CoFe-based MGs upon a minor Cu addition. The maximum indentation depth h_{in} exhibits a resembling loading-rate dependency as *E*. The h_{in} increases gradually with increasing loading rates for both Cu0 and Cu0.5 MGs. Compared with the non-Cu MG, the h_{in} of Cu0.5 is about 7% larger, demonstrating a pronounced creep deformation. It is consistent with the fact that a tiny Cu can significantly improve the compressive plasticity of CoFe-based bulk MGs [19]. These parameters are barely influenced by the loading rate when the loading rate is lower than 10 mN/s, which differs from the scenario at a higher loading rate. It demonstrates that the loading mode changes from a quasi-static mode into a low-velocity impact mode at a relatively high loading rate.

Fig. 3 shows the typical creep displacement - time curve of Cu0 and Cu0.5 MGs at different loading rates. It can be seen that the creep deformation becomes more pronounced with increasing loading rates. The maximum creep displacement rises from

Table 1
The fitting parameters of creep curves of Cu0 and Cu0.5 based on the Maxwell-Voigt model.

Alloy	Loading rate (mN s^{-1})	h_1 (nm)	τ_1 (s)	h_2 (nm)	τ_2 (s)	μ_0^{-1}(nm s^{-1})
Cu0	0.5	2.7 ± 0.6	1.8 ± 0.7	2.6 ± 0.5	13.8 ± 5.2	0.075 ± 0.004
	5	3.3 ± 0.3	1.3 ± 0.3	8.6 ± 0.4	19.8 ± 2.1	0.103 ± 0.005
	10	5.3 ± 0.3	1.2 ± 0.2	10.6 ± 0.5	22.2 ± 2.4	0.107 ± 0.007
	50	4.1 ± 0.3	1.0 ± 0.2	12.9 ± 0.7	23.5 ± 2.2	0.127 ± 0.016
	100	5.9 ± 0.3	0.9 ± 0.2	13.0 ± 0.8	24.7 ± 2.5	0.172 ± 0.009
Cu0.5	0.5	2.1 ± 0.3	0.5 ± 0.3	3.3 ± 0.3	15.4 ± 3.3	0.062 ± 0.004
	5	3.8 ± 0.3	0.6 ± 0.2	8.7 ± 0.3	16.2 ± 1.3	0.176 ± 0.004
	10	2.9 ± 0.3	1.0 ± 0.3	10.8 ± 0.5	22.1 ± 2.1	0.222 ± 0.007
	50	4.6 ± 0.3	1.4 ± 0.3	13.0 ± 0.9	26.6 ± 3.0	0.166 ± 0.010
	100	4.6 ± 0.2	0.6 ± 0.1	10.7 ± 0.4	18.5 ± 1.4	0.227 ± 0.005

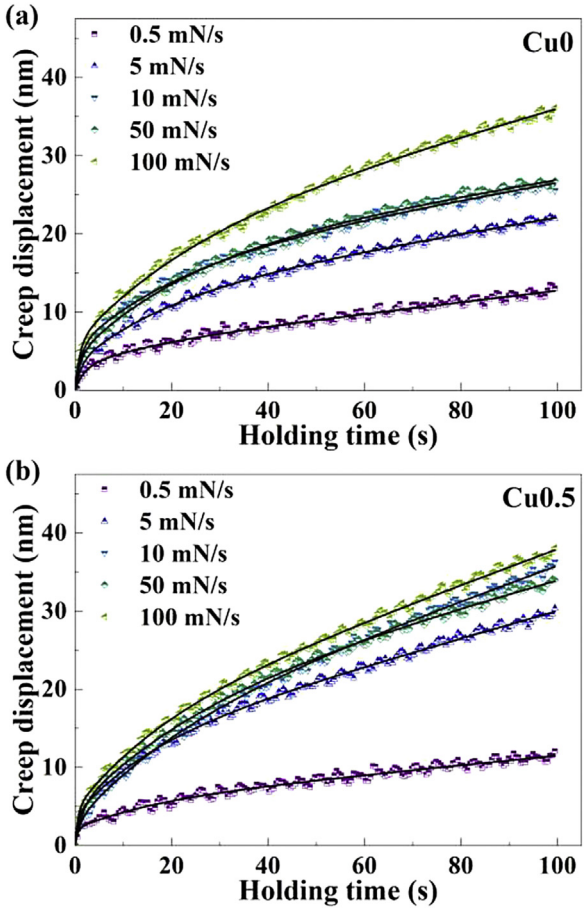

Fig. 3. Experimental and fitting creep curves of Cu0 (a) and Cu0.5 (b) MGs at different loading rates.

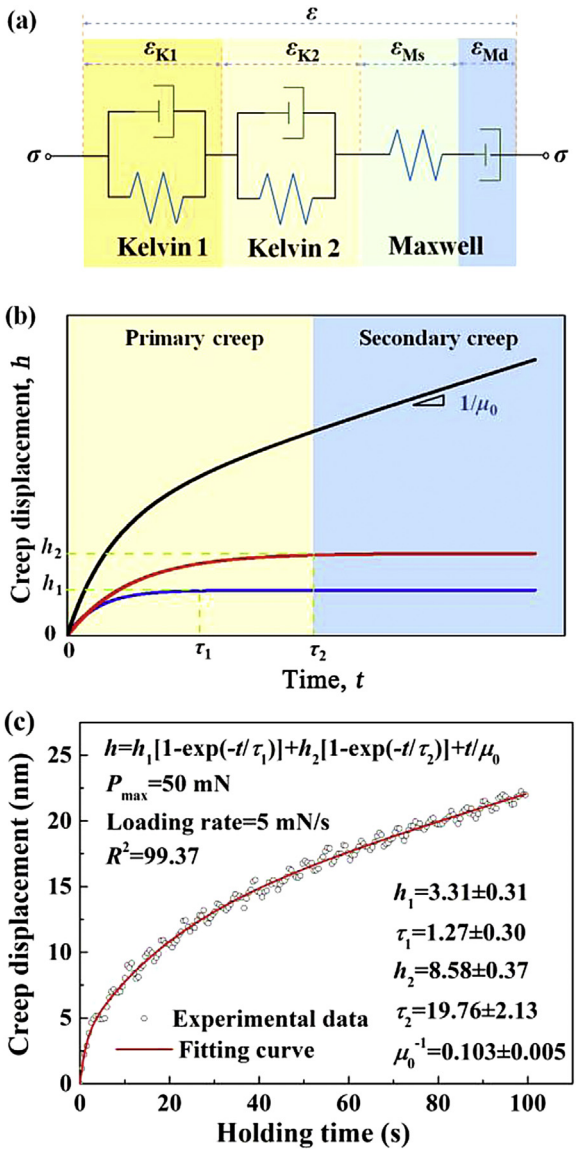

Fig. 4. (a) The Maxwell-Voigt model used for analyzing creep curves; (b) the schematic diagram of the *h*-*t* curve during the holding stage; (c) the typically fitted creep curve of Cu0 MG at a loading rate of 5 mN/s under a maximum load of 50 mN.

13 to 36 and 12 to 38 nm for Cu0 and Cu0.5 MGs, respectively. It slightly increases with the addition of Cu at a loading rate higher than 5 mN/s. In order to clarify the creeping process in detail, creep curves are analyzed by using the Maxwell-Voigt model that contains Maxwell units and Kelvin units connected mutually in series, as illustrated in Fig. 4(a). This model can well describe the creep deformation of viscoelastic materials during an indentation process [27,28]. As shown in Fig. 4(b), the creep displacement is set as 0 at t = 0. It means elastic strain ε_{Ms} that represents sudden strain before the first stage of anelastic deformation, i.e. the initial displacement, is assumed as 0. Therefore, the creep displacement without considering of elastic strain of Maxwell spring only contains the strain of the Maxwell dashpot ε_{Md} and the strain of the i-th Kelvin unit ε_{Ki}, which can be expressed by the following equation [4,27]:

$$h(t) = \sum_{i=1}^{n} h_i\,(1 - e^{-t/\tau_i}) + t/\mu_0 \qquad (1)$$

where h_i is the indentation depth, τ_i the characteristic relaxation time for the activation of the i-th anelastic Kelvin unit, t the experimental time during the holding segment, and μ_0 a constant

proportional to the viscosity coefficient of the Maxwell dashpot. As shown in Fig. 4(c), the creep displacement - time curve of CoFe-based MGs can be fitted successfully with Eq. (1), where the model includes one Maxwell unit and two Kelvin units, i.e., i = 2. Thus, the creep curve can be divided into two parts: the primary elastic component responding to a fast but decreasing strain rate, where two Kelvin units reflected by changes in h_i and τ_i play a major role in the strain rate; the secondary viscous component responding to a slow but constant strain rate μ_0^{-1}, where Maxwell dashpot plays a major role in determining the strain rate (Fig. 4(b)).

The fitting curves by using Eq. (1) under the frame of the Maxwell-Voigt model are plotted in Fig. 3. The values of the fitting parameters for creep curves at different loading rates, together with the standard error due to the fitting procedure, are included in Table 1. Fig. 5 displays fitting parameters at different loading rates. Both the primary elastic and secondary viscous components are dependent on the loading rate. The h_1 and h_2 increase sharply with increasing loading rates at a low loading rate, then almost keep a constant value at a loading rate higher than 10 mN/s. The τ_2 shows a similar loading-rate dependency. This phenomenon suggests a high loading-rate sensitivity of MGs under the quasi-static loading mode. The change tendency of τ_1 is different in two MGs at a low loading rate. The τ_1 of Cu0 decreases rapidly with increasing loading rates, while τ_1 of Cu0.5 increases at the first stage. It indicates that the structural evolution of Cu0.5 as a function of loading rates differs from that of Cu0. However, if we consider that the error bar of these fitting parameters that represent anelastic components is more than 10 %, particularly in the case of a very low loading rate e.g. 0.5 mN/s (the standard error is over 30 %), both h_i and τ_i are weakly affected by a minor Cu addition.

On the other hand, the value of μ_0 for Cu0 and Cu0.5 MGs dramatically decreases with the increase of loading rate at a quasi-static loading mode, as shown in Fig. 5(c). The μ_0 of Cu0.5 is much lower than that of Cu0 MG at the same rate, suggesting a significant decrease of viscosity. Compared with the resembling values of h_i and τ_i at high loading rates, a large difference in μ_0 between Cu0.5 and Cu0 can be found. It manifests that the addition of the Cu element has a strong impact on the viscoplastic deformation rather than the anelastic deformation of FeCo-based MGs. Cu0.5, thereby, is likely to undergo a much stronger viscoplastic deformation as compared with the Cu0 under the same loading condition.

As reported in previous studies [4,13], the anelastic component of the creep process can be described in terms of a relaxation time spectrum, which provides more details of the defect activation during the creep process. The isothermal relaxation spectra can be calculated by means of the following approximated expression [29]:

$$L(\tau) = \left[\sum_{i=1}^{n}(1+\frac{t}{\tau_i})\frac{h_i}{\tau_i}e^{-t/\tau_i}\right]\frac{A_0}{P_0 h_{in}}t\Big|_{t=2\tau} \quad (2)$$

where L is the spectrum intensity, A_0/P_0 the inverse of the hardness H, and h_{in} the maximum indentation depth as defined previously. Herein, h_i τ_i and t are the same parameters as derived in Eq. (1).

Fig. 6 presents relaxation time spectra of Cu0 and Cu0.5 MGs at different loading rates, all of which exhibit two separate relaxation peaks. It can be found that when the loading rate increases from 0.5 to 100 mN/s, the intensity of both first and secondary peaks in relaxation spectra of Cu0 increases remarkably, as shown in Fig. 6(a). This phenomenon has also been observed in U-based MGs [27], which reveals that more free volumes or defects are activated at a higher loading rate. The characteristic relaxation time of the first peak of Cu0 MG decreases gradually with increasing loading rates, while that of the secondary peak increases instead. It seems that defects in Cu0 MG corresponding to the first peak with a short relaxation time intend to be simulated at a higher loading rate, in the meantime the activation of defects that relates to the secondary relaxation process with a longer relaxation time prefers to occur. This result indicates that the defects with large size are more likely to be provoked at a low-velocity impact mode for the non-Cu MG. The relaxation spectra of Cu0.5 MG show a similar change tendency, see Fig. 6(b). However, the characteristic relaxation time, as well as the intensity of relaxation peaks, is less sensitive to the loading-rate. The significant fluctuation of the characteristic relaxation time coincides with the structural heterogeneity ranging from several angstroms to dozens of nanometers

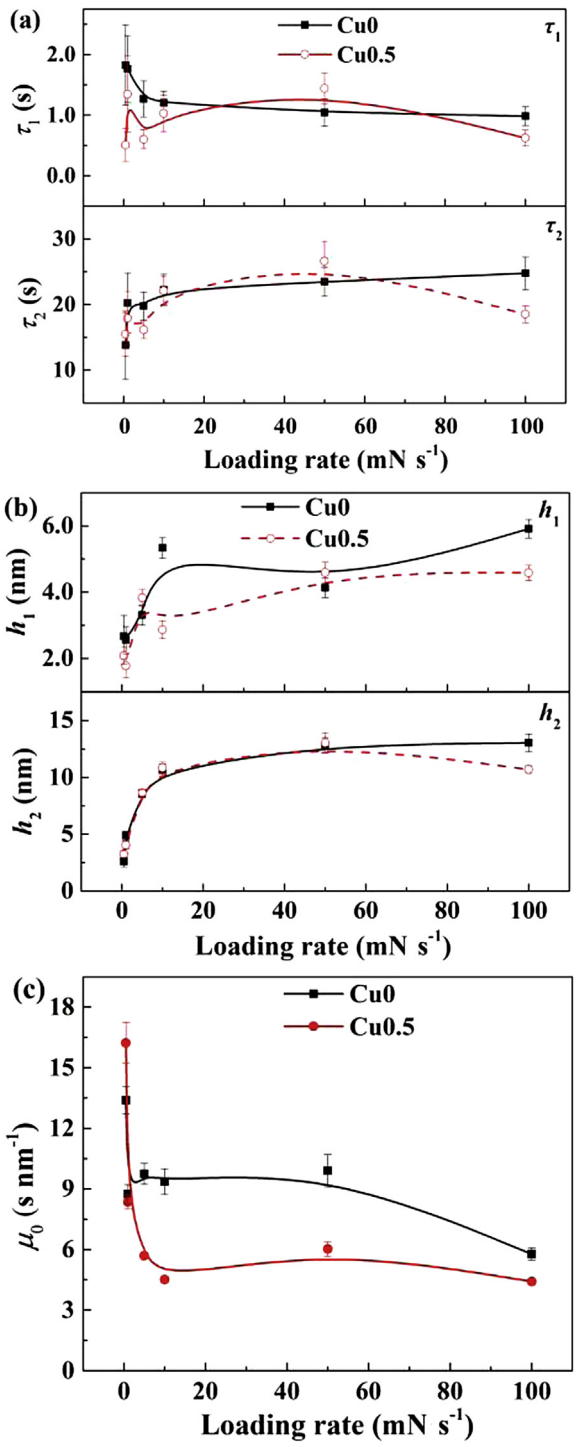

Fig. 5. The characteristic relaxation time τ_i (a), indentation depth h_i (b), and viscosity constant μ_0 (c) as a function of the loading rate.

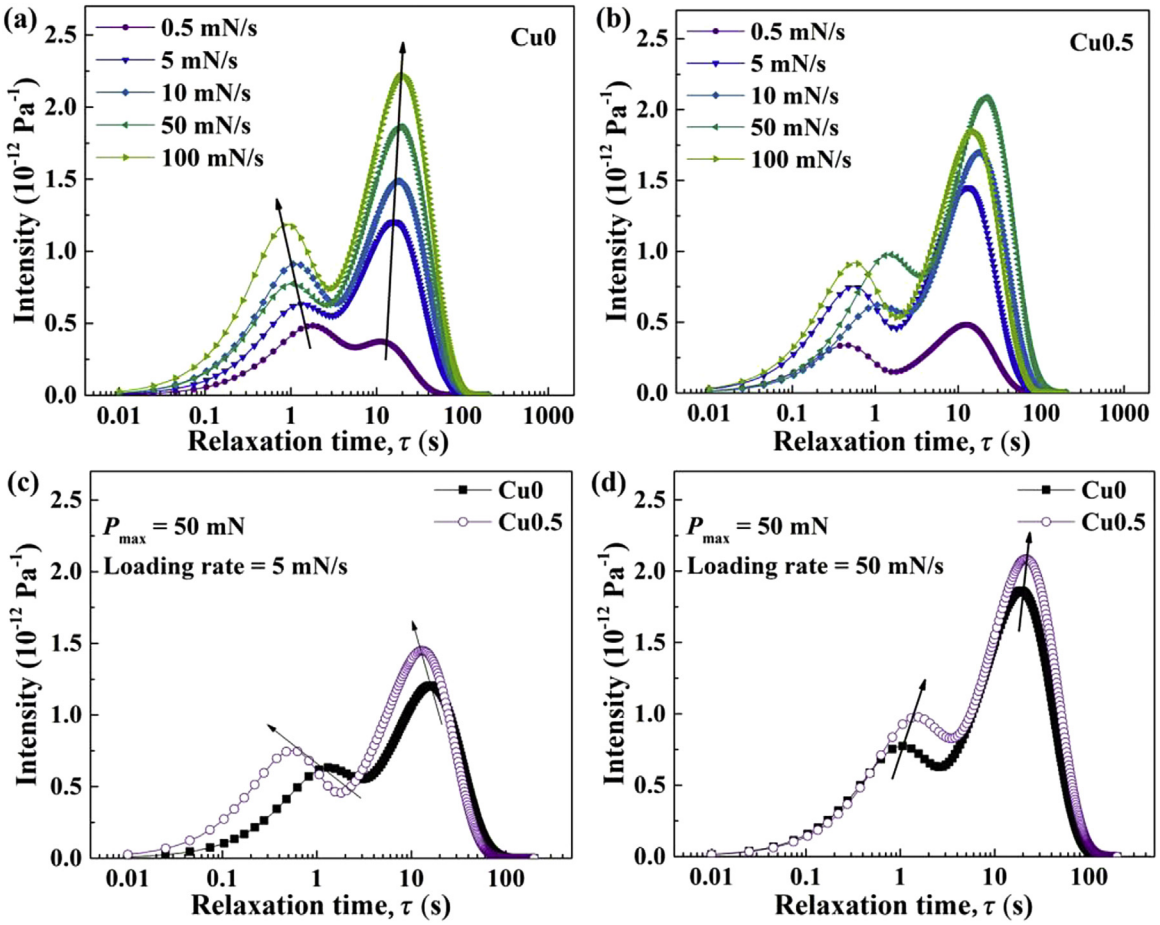

Fig. 6. Relaxation time spectra of Cu0 (a) and Cu0.5 (b) MGs based on the anelastic part of their creep curves with a maximum load of 50 mN at different loading rate; the relaxation spectra of Cu0 and Cu0.5 MGs at the loading rate of 5 mN/s (c) and 50 mN/s (d).

found in Cu-doped FeCo-based MGs [26]. It is also noticed that the secondary peak reaches the highest intensity at the loading rate of 50 mN/s. The intensity sharply drops at a higher loading rate of 100 mN/s. This abnormal variation may be attributed to the fact that the number of defects activated during the creep process reaches the maximum value at the loading rate of 50 mN/s.

The coexistence of hard and soft phases has been observed in many MGs including our studied system [14,26,30–32]. According to the two-phase model [33], the first peak of relaxation spectra with a short relaxation time τ_1 can stand for the response of hard regions with a strongly bonded configuration, while the secondary peak with a longer relaxation time τ_2 can stand for soft regions with a weakly atomic bonding. The intensity of first and secondary peaks in relaxation spectra slightly raises after doping 0.5 at.% Cu into CoFe-based MGs and the characteristic relaxation times of both two peaks show an obvious shift towards a shorter time region at the loading rate of 5 mN/s, see Fig. 6(c). It indicates that the addition of a tiny Cu makes the activation of defects at both soft and hard regions easier. This scenario can be described well in the schematic diagram of Fig. 7. Compared with Cu0, the defects with small size are inclined to be activated in the Cu0.5 MG. The number of activated defects is slightly larger than that of Cu0 at a low loading rate, see Fig. 7(b). Moreover, the defect in soft regions tends to be interconnected during the plastic flow process. This may result in the high deformability of Cu-doped MGs with multiple shear bands at a quasi-static loading mode as reported in the compressive experiment [19]. The relaxation spectra show a dissimilar performance at the low-velocity impact mode, for example, at a loading rate of 50 mN/s as shown in Fig. 6(d). The characteristic relaxation time τ_1 and τ_2 show a slight shift towards a longer relaxation time upon 0.5 at. % Cu addition, and the intensity of the two relaxation peaks increase. It means that more defects with a relatively large size at soft regions are activated for Cu0.5 MG as compared with Cu0 MG, see the schematic diagram as shown in Fig. 7(c). It is in agreement with the observation in our previous work that free volume is more likely to generate at the continuous weakly-bonded soft region during the plastic deformation of the Cu-doped MG [14,26]. The increase of the number of activated defects at both soft and hard regions upon Cu doping can prevent the stress concentration inside a single primary shear band or at the tip of the crack, which is in favor of the nucleation of secondary shear bands/microcracks, see Fig. 7(c). Such an energy dissipation process due to the defect activation effectively promotes the plastic flow of MGs.

4. Conclusion

The nanoindentation creep of $[(Co_{0.7}Fe_{0.3})_{0.68}B_{0.219}Si_{0.051}Nb_{0.05}]_{100-x}Cu_x$ (x = 0, 0.5) MGs at room temperature was investigated under the frame of Maxwell-Voigt model. We found that for two MGs, E and h_{in} increases gradually with increasing loading rates, while H decreases slightly, at a loading rate higher than 10 mN/s. It demonstrates that the mechanical properties of MGs are sensitive to both loading-rate and the loading mode. As compared with Cu0, the E and H of Cu0.5 are much smaller due to the softening upon a minor Cu addition. It is consistent with the much larger maximum indentation depth, h_{in} of Cu0.5 alloy than that of the non-Cu MGs. The creep curves at different loading rates can be described well by using the Maxwell-Voigt model with two Kelvin units

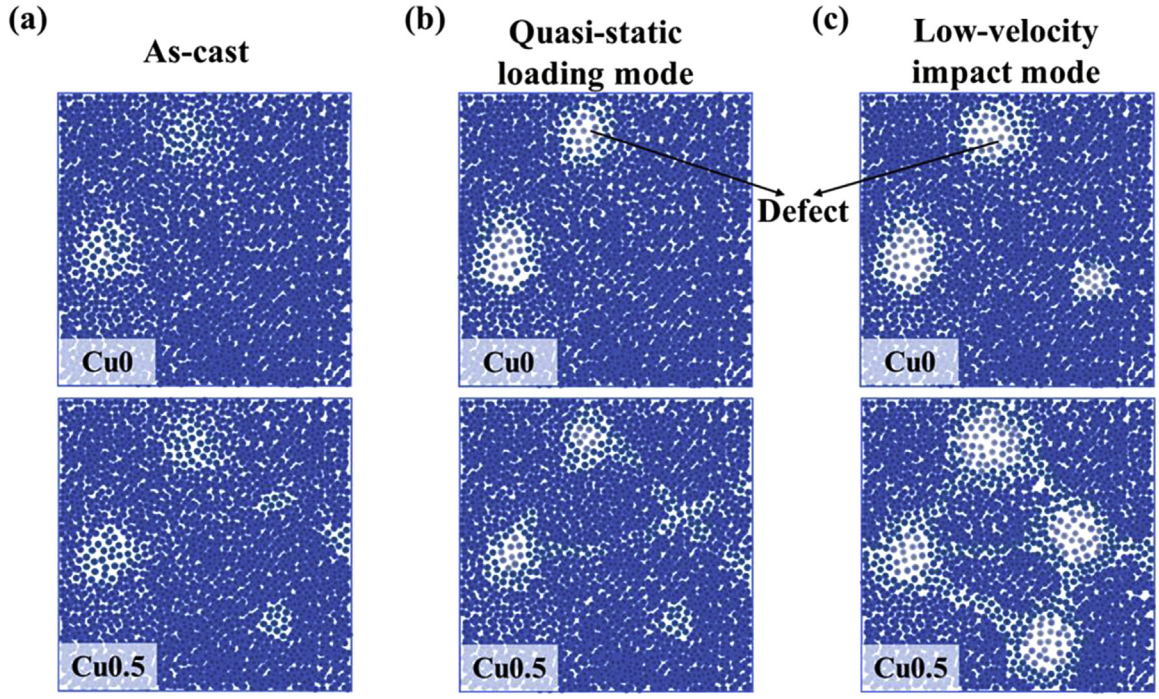

Fig. 7. A schematic diagram for the distribution of defects in Cu0 and Cu0.5 MGs at the as-cast state (a), quasi-static loading mode (b), and low-velocity impact mode (c).

and one Maxwell unit. It is found that the viscosity is obviously reduced during the viscoplastic deformation in the Cu-doped MG, according to the decrease of μ_0. Herein, Cu0.5 MG undergoes more pronounced viscoplastic flow during the creep deformation. The two characteristic peaks in relaxation time spectra relate to two kinds of defects activated during deformation. At a quasi-static loading mode, the defect with a small size is more likely to be activated in the Cu0.5 MG, as indicated by a shift of the relaxation time τ_1 and τ_2 toward a shorter time region. While at a low-velocity impact mode, more defects at both hard and soft regions were propagated in Cu0.5 MG, corresponding to a more intense first and secondary peaks in the relaxation spectra of Cu0.5 MG. The activation of a large number of defects with different sizes along with the pronounced viscoplastic deformation in Cu0.5 promotes more energy dissipation at the tip of microcracks or inside the primary shear band and stimulates the generation of secondary shear bands, which leads to the improved plasticity of Cu-doped MGs.

Acknowledgements

This work was supported financially by the Natural Science Foundation of Jiangsu Province, China (No. BK20171354), the National Natural Science Foundation of China (Nos. 51631003 and 51601038), the Key Basic and Applied Research Program of Guangdong Province, China (No. 2019B030302010), the Fundamental Research Funds for the Central Universities (No. 2242020K40002), the Jiangsu Key Laboratory for Advanced Metallic Materials (No. BM2007204).

References

[1] W.L. Johnson, MRS Bull. 24 (2013) 42–56.
[2] C. Schuh, T. Hufnagel, U. Ramamurty, Acta Mater. 55 (2007) 4067–4109.
[3] D.D. Xu, B.L. Zhou, Q.Q. Wang, J. Zhou, W.M. Yang, C.C. Yuan, L. Xue, X.D. Fan, L.Q. Ma, B.L. Shen, Corros. Sci. 138 (2018) 20–27.
[4] A. Castellero, B. Moser, D.I. Uhlenhaut, F.H.D. Torre, J.F. Löffler, Acta Mater. 56 (2008) 3777–3785.
[5] Y.H. Chen, J.C. Huang, L. Wang, T.G. Nieh, Intermetallics 41 (2013) 58–62.
[6] B. Shen, H. Men, A. Inoue,Appl. Phys. Lett. 89 (2006), 101915.
[7] L. Zhang, P. Yu, H. Cheng, H. Zhang, H. Diao, Y. Shi, B. Chen, P. Chen, R. Feng, J. Bai, Q. Jing, M. Ma, P.K. Liaw, G. Li, R. Liu, Metall. Mater. Trans. A 47 (2016) 5871–5875.
[8] A. Concustell, J. Sort, A.L. Greer, M.D. Baró,Appl. Phys. Lett. 88 (2006), 171911.
[9] V. Ocelík, K. Csach, A. Kasardová, V.Z. Bengus, Mater. Sci. Eng. A 226 (1997) 851–855.
[10] J.J. Pang, M.J. Tan, K.M. Liew, C. Shearwood, Phys. B 407 (2012) 340–346.
[11] Y. Ma, G.J. Peng, Y.H. Feng, T.H. Zhang, J. Non-Cryst. Solids 465 (2017) 8–16.
[12] C.C. Hays, C.P. Kim, W.L. Johnson, Phys. Rev. Lett. 84 (2000) 2901–2904.
[13] P. Gong, J. Jin, L. Deng, S. Wang, J. Gu, K. Yao, X. Wang, Mater. Sci. Eng. A 688 (2017) 174–179.
[14] C.C. Yuan, Z.W. Lv, C.M. Pang, W.W. Zhu, X.L. Wang, B.L. Shen, J. Alloys Compd. 806 (2019) 246–253.
[15] F. Xu, Z.L. Long, X.H. Deng, P. Zhang, Trans. Nonferrous Met. Soc. China 23 (2013) 1646–1651.
[16] Y.J. Huang, J. Shen, Y.L. Chiu, J.J.J. Chen, J.F. Sun, Intermetallics 17 (2009) 190–194.
[17] X. Li, H. Kato, K. Yubuta, A. Makino, A. Inoue, Mater. Sci. Eng. A 527 (2010) 2598–2602.
[18] C.L. Zhao, C.C. Dun, Q.K. Man, B.L. Shen, Intermetallics 32 (2012) 408–412.
[19] G.L. Zhang, Q.Q. Wang, C.C. Yuan, W.M. Yang, J. Zhou, L. Xue, F. Hu, B.A. Sun, B.L. Shen, J. Alloys Compd. 737 (2018) 815–820.
[20] Z.Z. Li, A. Wang, C.T. Chang, Y.G. Wang, B.S. Dong, Intermetallics 54 (2014) 225–231.
[21] F.L. Kong, H. Men, M.X. Zhang, T.C. Liu, G.Q. Xie, B.L. Shen, Appl. Phys. A 108 (2012) 211–215.
[22] J.S. Blazquez, C.F. Conde, A. Conde, Appl. Phys. A 76 (2003) 571–575.
[23] Y. Wu, H.X. Li, J.E. Gao, H. Wang, X.J. Liu, M.K. Miller, H. Bei, Y.F. Gao, Z.P. Lu, J. Alloys Compd. 688 (2016) 822–827.
[24] A. Takeuchi, A. Inoue, Mater. Trans. 46 (2005) 2817–2829.
[25] M. Heggen, F. Spaepen, M. Feuerbacher,J. Appl. Phys. 97 (2005), 033506.
[26] C.C. Yuan, Z.W. Lv, C.M. Pang, X.L. Wu, S. Lan, C.Y. Lu, L.G. Wang, H.B. Yu, J.H. Luan, W.W. Zhu, G.L. Zhang, Q. Liu, X.L. Wang, B.L. Shen, J. Alloys Compd. 798 (2019) 517–522.
[27] H.B. Ke, P. Zhang, B.A. Sun, P.G. Zhang, T.W. Liu, P.H. Chen, M. Wu, H.G. Huang, J. Alloys Compd. 788 (2019) 391–396.
[28] B.G. Yoo, I.C. Choi, Y.J. Kim, U. Ramamurty, J.I. Jang, Mater. Sci. Eng. A 577 (2013) 101–104.
[29] J.D. Ferry, Viscoelastic Properties of Polymers, third ed., John Wiley & Sons, New York, 1980.
[30] X.H. Du, J.C. Huang, K.C. Hsieh, Y.H. Lai, H.M. Chen, J.S.C. Jang, P.K. Liaw,Appl. Phys. Lett. 91 (2007), 131901.
[31] G. Wu, K.C. Chan, L. Zhu, L. Sun, J. Lu, Nature 545 (2017) 80–83.
[32] P. Tsai, K. Kranjc, K.M. Flores, Acta Mater. 139 (2017) 11–20.
[33] J.C. Ye, J. Lu, C.T. Liu, Q. Wang, Y. Yang, Nat. Mater. 9 (2010) 619–623.